Polar Biol (2014) 37:1579–1588
DOI 10.1007/s00300-014-1543-5

ORIGINAL PAPER

Vegetation abundance on the Barton Peninsula, Antarctica: estimation from high-resolution satellite images

Jung-Il Shin · Hyun-Cheol Kim · Sang-Il Kim · Soon Gyu Hong

Received: 5 November 2013 / Revised: 1 July 2014 / Accepted: 2 July 2014 / Published online: 19 July 2014

Abstract Polar biodiversity should be monitored as an indicator of climate change. Biodiversity is mainly observed by field survey although this is very limited in broad inaccessible polar regions. Satellite imagery may provide valuable data with less bias, although spatial, spectral, and temporal resolutions are limited for analyzing biodiversity. The present study has two objectives. The first is constructing a first-ever vegetation map of the entire Barton Peninsula, Antarctica. The second is developing a monitoring method for long-term variation of vegetation, based on satellite images. Dominant mosses and lichens are distributed in small and sparse patches, which are limited to analysis using high-resolution satellite images. A sub-pixel classification method, spectral mixture analysis, is applied to overcome limited spatial resolution. As a result, vegetation shows high abundance along the southeastern shore and low-to-medium abundance in the nearly snow-free inland area. Even though spatial patterns of vegetation were almost invariant over 6 years, there was interannual variation in abundance aspects because of meteorological conditions. Therefore, extensive and long-term monitoring is needed for aspects of distribution and abundance. The present results can be used to design field surveys and monitor long-term variation as elementary data.

Keywords Abundance · Vegetation · Antarctica · Satellite · Spectral mixture analysis

J.-I. Shin · H.-C. Kim (✉) · S.-I. Kim · S. G. Hong
Korea Polar Research Institute, KIOST, 26 Songdomirae-ro, Yeonsu-gu, Incheon 406-840, South Korea
e-mail: kimhc@kopri.re.kr

Introduction

Vegetation in polar regions is adapted to an extreme environment and must respond rapidly to climate change to survive (Kennedy 1993; Robinson et al. 2003). Recently, severe climate change in the maritime Antarctic area around the Antarctic Peninsula has affected terrestrial biodiversity including vegetation (Sancho and Pintado 2004; Bergstrom et al. 2006; Convey 2011; Torres-Mellado et al. 2011). The resulting adaptation and changes of polar vegetation may be used as an indicator of climate change (Green et al. 2011). Changes of biodiversity may have a positive effect on habitat productivity and biomass as well as on populations of individual species at short- and mid-term timescales. However, in the long term, biodiversity changes may disrupt the ecosystem by increasing the abundance of non-native species (Convey 2011). Therefore, changes of polar vegetation should be observed as an index used to monitor climate change, such as the distribution and variation of species in terms of biodiversity.

Many studies have observed biodiversity in maritime Antarctica (including King George Island) via field surveys (Furmanczyk and Ochyra 1982; Barcikowski and Gurtowska 1999; Poole et al. 2001; Kim et al. 2006, 2007; Pereira et al. 2007; Victoria et al. 2009). Field surveys have limitations because they do not allow observation of a broad area and variations occur during collection of data time series and extensive surveys require substantial labor, time, and cost. Most of all, human activity during field surveys may permanently destroy portions of the very slowly growing polar vegetation. These factors give field survey data significant uncertainty, making it difficult to quantitatively analyze variations of vegetation and the effect of climate change over a broad area (Robin et al. 2011).

Satellite imagery can provide valuable data, allowing researchers to overcome the inherent limitations of field surveys by observing a broad area simultaneously and frequently with less bias. Many studies have surveyed polar vegetation using various remote sensing data and analytical techniques. Most focused on vegetation in Arctic tundra (Stow et al. 2004; Frohn et al. 2005; Raynolds et al. 2006, 2008; Laidler et al. 2008; Bhatt et al. 2010). Relatively few investigations have targeted Antarctic vegetation through estimating vegetated areas, and these were not properly validated because of a lack of in situ reference data (Murray et al. 2010; Fretwell et al. 2011).

Mid- or low-resolution satellite images such as from AVHRR, MODIS, Landsat, and SPOT have mainly been used to observe vegetation in polar regions (Stow et al. 2004; Bhatt et al. 2010; Fretwell et al. 2011). However, the flora of polar region tundra is predominantly mosses and lichens, which usually have small size and height and irregular distributions and community-level ground coverage (Raynolds et al. 2006). In this environment, mid- or low-resolution images have limited use in analysis of vegetation spatial coverage or distribution. Therefore, high-resolution imagery is more appropriate for observation and analysis of polar vegetation (Murray et al. 2010).

Selection or design of classifiers is important for improved vegetation mapping in a given environment because there are no superior image classifiers for all applications (Xie et al. 2008). Supervised or unsupervised classification methods have generally been used in previous studies to detect or classify vegetation from satellite images. Moreover, many studies have used vegetation indices such as the normalized difference vegetation index (NDVI) (Murray et al. 2010; Fretwell et al. 2011; Robin et al. 2011). However, hard classification (such as supervised or unsupervised classification) methods that classify a pixel as a material or land-cover type are not appropriate. Because tundra consists of sparse vegetation communities, they are mixed with neighboring rock, soil, and snow within areas smaller than the pixel size of high-resolution satellite imagery. Additionally, supervised classification usually needs a sufficient number of samples for training and validation, but extensive field surveys are limited in broad, inaccessible areas. Therefore, soft classification methods, which can facilitate estimation of a fraction of surface materials at sub-pixel scale, are needed to accurately estimate a vegetated area in polar regions (Théau et al. 2005).

The objective of this study is satellite-based estimation of simultaneous vegetation abundance and distributions across Barton Peninsula, King George Island. First, we constructed for the first time an elementary vegetation map. Second, we developed a monitoring method for long-term variation of the vegetation, based on the satellite imagery. Two high-resolution satellite images were used to confirm consistency of the method or results. A spectral mixture analysis (SMA) method was used to estimate vegetation abundance, because of sparse communities smaller than pixel size.

Study area and data

Barton Peninsula

The study area is the Barton Peninsula of King George Island, where King Sejong Station is located (Fig. 1). The island is between 57°40′W–59°00′W and 61°50′S–62°15′S and covers about 2,600 km^2, making it the largest of the South Shetland Islands. Almost all the land is covered with glaciers, except in coastal regions where geologically dominated environments remain poor in organic material and nutrients. However, the relatively moderate maritime climate allows the distribution of various species and facilitates the transport of nutrients into the area, such as wind-blown and precipitation-borne materials and guano (Bokhorst et al. 2007). The Barton Peninsula is at the southwestern part of King George Island and has an area of about 10 km^2 (4 × 3 km) and average elevation 150 m. Meteorological records from King Sejong Station have been collected since 1988, indicating an average annual temperature −1.8 °C and average summer temperature 1.6 °C (December through February). Relative humidity averages 89 %, with an average 437 mm of precipitation annually (Lee et al. 1997; Chung et al. 2004). Flora on the peninsula is predominately mosses, lichens and vascular plants (Kim et al. 2006; Lee et al. 2008), in generally small (sub-meter), sparse and irregular patches.

Satellite and field data

Two types of satellite images were used, KOMPSAT-2 (KOrea Multi-Purpose SATellite-2) multispectral and QuickBird multispectral (Fig. 1). Table 1 provides specifications of these types. These high-resolution satellite images typically have a spatial resolution of several meters, which is adequate for estimating the abundance of sparse vegetation. Further, these images have a near-infrared (NIR) band, which is essential to effectively observe vegetative conditions. In our study, a sub-image of each satellite image was used to study the land area. The images were acquired with different sun and sensor geometries (Table 1), with varying shade areas. Union areas of shadow were masked out from the two images for reasonable comparison between their SMA results. Shadow was detected with a supervised classifier (maximum likelihood), in which training samples were collected by visual interpretation of each image.

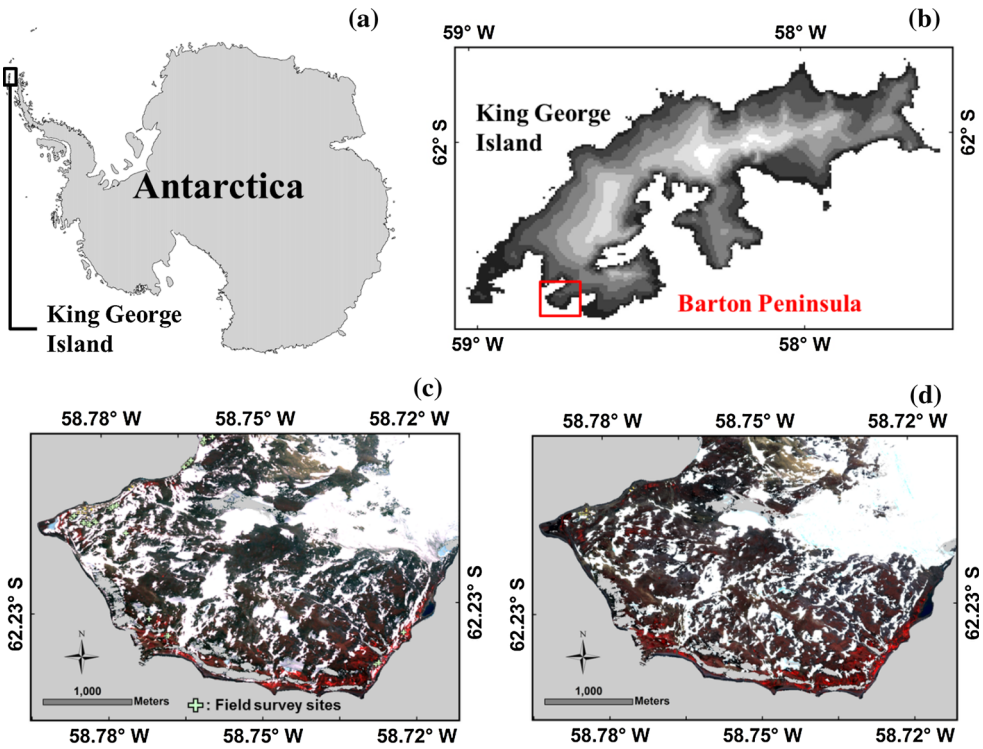

Fig. 1 Vicinity map and satellite images of study area on Barton Peninsula, King George Island, Antarctica. **a**, **b** are locations of King George Island and Barton Peninsula, respectively, **c** is KOMPSAT-2 image from February 24, 2012, and **d** is QuickBird image from December 6, 2006. Vegetation is shown in red, based on color composite of bands (RGB = NIR R G). *Green crosses* indicate locations of 29 selected field survey sites in 2012

Table 1 Specifications of satellite imagery analyzed in this study (*B* blue, *G* green, *R* red, *NIR* near-infrared)

Sensor	KOMPSAT-2	Quickbird
Acquisition date	2012. 02. 24	2006. 12. 06
Spatial resolution	4 m	2.4 m
No. of band	4 (B, G, R, NIR)	4 (B, G, R, NIR)
Swath width	15 km	16.5 km
Digital quantization	10 bit	11 bit
Sun elevation angle	37°	46°
Sun azimuth angle	10°	41°
Sensor viewing angle (along track)	0°	−6°
Across track	+23°	+6°

Field surveys along the coast from January 7 to February 8, 2012, included measurements of vegetation coverage. This coverage was measured by visual interpretation of natural color photos taken of 50 × 50 cm quadrats (10 × 10 cm for each sub-quadrat; Fig. 2). When a sub-quadrat was covered by more than half with vegetation, it was counted as vegetated. Vegetation coverage was recorded with the fraction of vegetated sub-quadrats to total number of sub-quadrats (25) using 10 % divisions. Among a total of 88 field survey sites, only 29 were selected for validation because those were concurrently snow-free, shadow-free, and "homogeneous" in the KOMPSAT-2 (Feb. 2012) image. Here, homogeneous site means that pixels had similar brightness (or color) and cover over at least 12 × 12 m (3 × 3 pixels), with consideration of the KOMPSAT-2 image spatial resolution. The 29 selected sites included predominant species (lichen and moss) with even vegetation coverage, although a small number of field survey sites were selected relative to the total number of the site. The locations of selected validation sites are shown by green crosses in Fig. 1.

Methods

SMA was used to estimate vegetation abundance for every pixel of each satellite image. SMA permits estimation of fractions of each material within each image pixel, which is assumed to be a mixture of certain materials such as vegetation, rock, and snow (the area of each pixel is not expected to be covered by pure material). The vegetated area is mixed with a background of soil and rocks, because of the three-dimensional structure of vegetation. For the preprocessing of SMA, minimum noise fraction (MNF) transformation and pixel purity index (PPI) methods (or algorithms) were used to collect endmembers (details in sub-section on endmember collection), which are defined as pixels with uniform coverage of plants or other material. Figure 3 shows the SMA image processing procedure, and each step is explained in the following sub-sections, with examples based on the KOMPSAT-2 image.

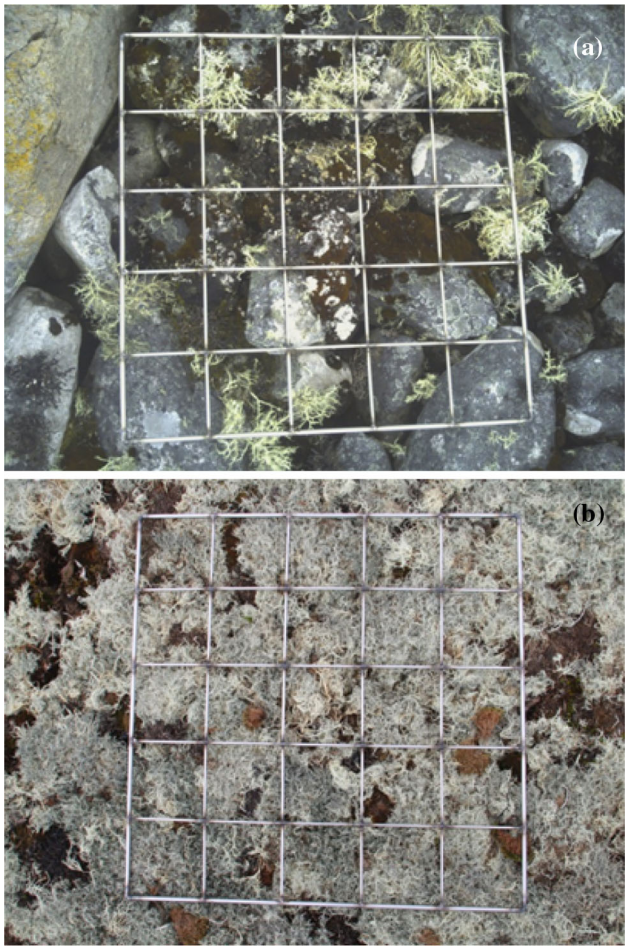

Fig. 2 50 cm × 50 cm quadrats (10 cm × 10 cm for each quadrat) used to survey vegetation abundance and species composition. **a** 60 % coverage with mixed flora (lichen and moss), **b** 100 % coverage with one species (lichen)

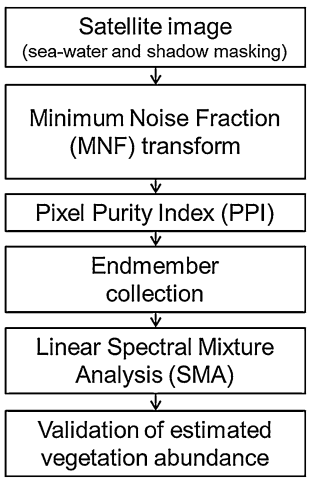

Fig. 3 Procedure used to estimate vegetation abundance

MNF transformation

Generally, principal component analysis (PCA) transformation is widely used to reduce the dimensionality of high-dimensional data such as multispectral images. As an advanced method, MNF transformation is used to simultaneously reduce both dimensionality and noise. This is a well-known preprocessing method for hyperspectral images of high dimensionality and high noise levels (Green et al. 1988; Jensen 2005). An MNF transform involves the following two steps of PCA analysis (Chen et al. 2003). First, data are decorrelated and noise is rescaled. As a result, noise has unit variance and no band-to-band correlation. Then, coherent MNF eigen-images and noise-dominated MNF eigen-images are created through a second PCA.

We used MNF instead of PCA to enhance radiometric quality of the KOMPSAT-2 image, as with IKONOS and QuickBird (Kim et al. 2012). Figure 4 shows four MNF eigen-images produced by MNF transformation of a KOMPSAT-2 image. Principle components (PCs) have high brightness values in each MNF band. PCs of the first (Fig. 4a), second (Fig. 4b) and third (Fig. 4c) MNF bands are represented by higher (brighter) values for: (a) low-albedo objects such as rock, soil, and water (b) mid-range albedo objects, which include areas of vegetation with some shaded snow, and (c) high-albedo objects, which included snow areas, respectively. By interpretation of MNF bands, the study area had three PCs with spectral characteristics of bare surfaces (rock, soil, and water) with low-albedo, vegetation with mid-albedo, and snow with high-albedo. The fourth MNF band presented bright pixels along edges between two land-cover (material) types without a specific PC, which may be assumed a noise component. Therefore, this band is excluded from further analysis.

Pixel purity indexing

The PPI represents spectral purity of each pixel using a relative value. To determine purity, pixels of coherent MNF eigen-images are repeatedly projected onto n-dimensional scatter plots (Jensen 2005). In each projection, most of the extreme pixels are noted. Therefore, pixels with high values are candidate endmembers in the PPI image. We determined optimum numbers of iteration and thresholds of noted values experimentally.

Endmember collection

An endmember is defined as the spectral signal of pure material for those pixels with uniform coverage of plants or

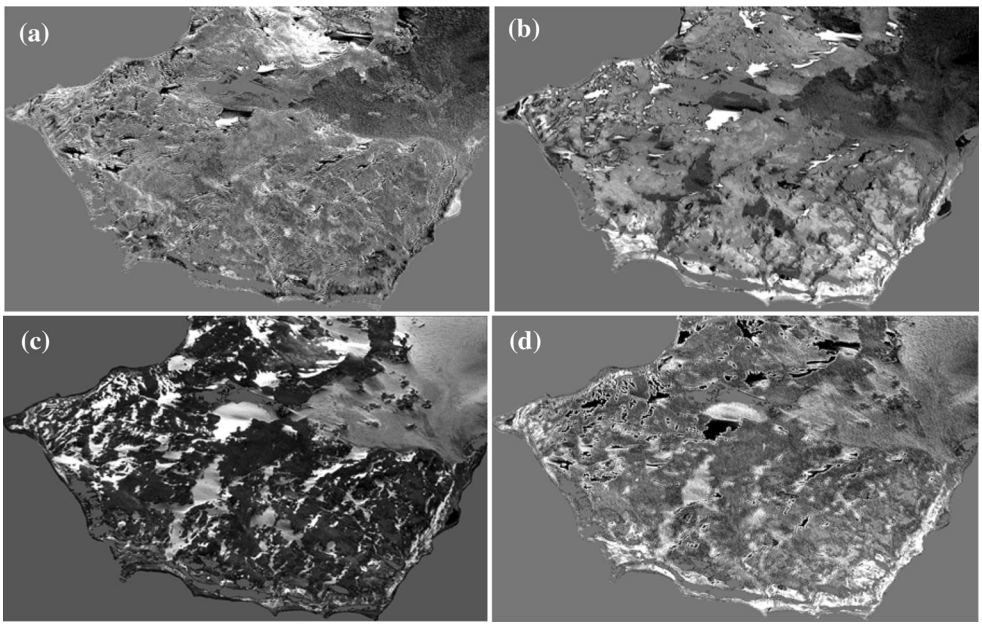

Fig. 4 MNF transformed bands from a KOMPSAT-2 image; MNF bands 1–3 have higher values for principal components (low-, middle-, and high-albedo objects), respectively, and MNF band 4 has a higher value for noise or edge of different cover types. **a** MNF band 1 (low-albedo objects: rock, soil, and water), **b** MNF band 2 (middle-albedo objects: vegetation and some shaded snow), **c** MNF band 3 (high-albedo objects: snow), **d** MNF band 4 (noise)

other material. An endmember could be an extremely pure pixel in the image, which can be determined by PPI analysis. Endmember candidates (pixels) are presented as points based on 2D projection of MNF bands, and endmembers are always located in an extreme area. We defined three materials as endmembers, snow, vegetation, and bare surface (rock/soil and water). Another source of an endmember could be field-measured spectra or spectral libraries, although we collect endmembers from each image itself. Each image had the same radiometric scale.

Spectral mixture analysis

Generally, the area of each pixel could be assumed to be composed of a mixture of various materials. Based on this assumption, the spectral signal of a pixel was defined as the sum of the weighted signal of endmembers by the fraction present in a pixel (Eq. 1). Therefore, SMA can estimate sub-pixel information (abundance) using an inverse calculation (Okin et al. 2001).

$$R_{\text{mix}} = f_A \times R_A + f_B \times R_B + f_C \times R_C + \varepsilon \quad (1)$$

where R is the spectral signal of each endmember or mixed pixel, f is the fraction (abundance) of each endmember in a pixel, A–C are each endmember, and ε is error. The fraction of each endmember may be estimated inversely with known variables (R_{mix}, R_A, R_B, and R_C). In our study, SMA was implemented with three endmembers (snow, vegetation, and bare surface) for three MNF bands. ENVI 4.8 software (Exelis Inc., McLean, VA, USA) was used for SMA, in which we did not use constraints to converge the error to zero as much as possible.

Validation

Field-measured vegetation abundance data were used to validate estimated vegetation abundance. For the KOMPSAT-2 image, 29 sites were used to compare estimated (SMA) vegetation abundance with measured (field survey) abundance. For the QuickBird image, estimated vegetation abundance was compared with vegetation coverage from a vegetation map that covered 0.4 km^2 around King Sejong Station (Kim et al. 2007) because of the lack of in situ field data. The vegetation map was generated with field survey data collected from 2001 to 2003.

Results

Abundance estimation from KOMPSAT-2 (February 2012)

Abundances of endmembers were estimated using a KOMPSAT-2 image from February 2012. Figure 5 shows abundance images of (a) vegetation, (b) bare surface, and (c) snow, with gray scale (0–1). Vegetation covered 34 % of

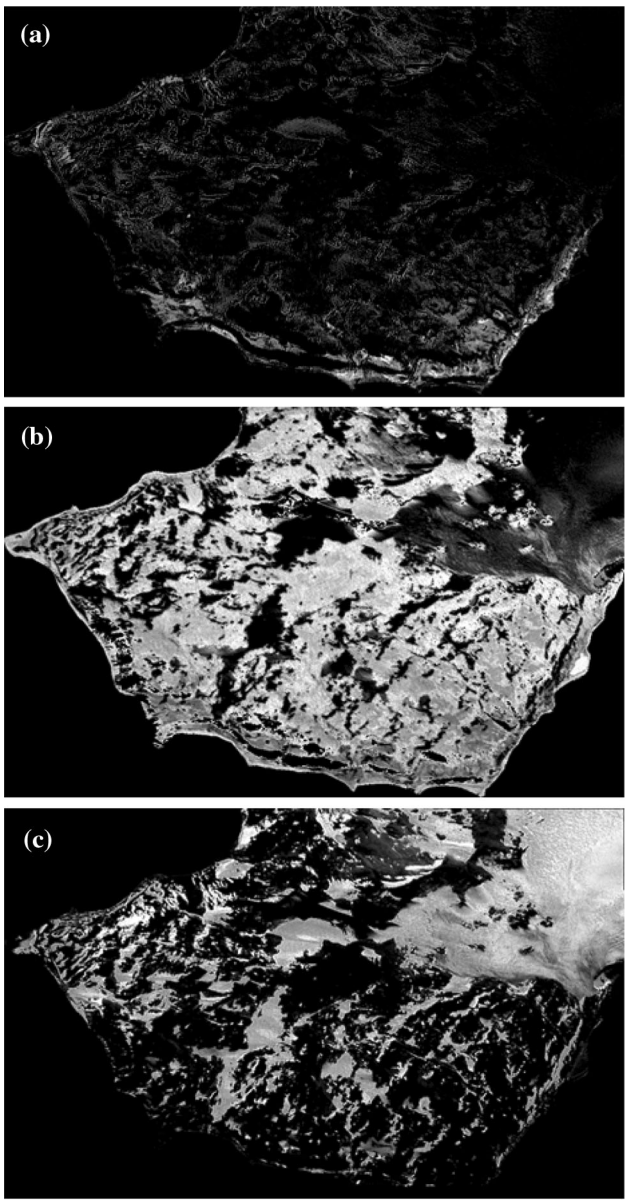

Fig. 5 Estimated abundance image from a KOMPSAT-2 image acquired in 2012 as a linear scale 0–1. **a** Vegetation, **b** bare surface, **c** snow

the entire area (Table 2). Vegetation was very abundant along the southeastern shore. Most snow-free areas had some vegetation in the mountainous inland areas, although most of these areas have not been surveyed. Bare surface (including rock, soil, and water) had 37 % abundance. Bare surface was distributed broadly in nearly snow-free areas, because rock and soil were mixed with sparse vegetation or exposed without vegetation. Snow showed 29 % abundance, with a massive glacier covering almost all the northeast peninsula. Large and small patches of snow covered other regions.

Vegetation coverage data from the 29 field survey sites were used to validate the estimated vegetation abundance

Table 2 Estimated abundance (%) of each endmember based on KOMPSAT-2 and QuickBird images

Endmember	KOMPSAT-2 (2012) (%)	Quickbird (2006) (%)	Difference (2006–2012) (%)
Vegetation	34.2	37.0	+2.8
Bare surface	37.0	42.3	+5.3
Snow	28.8	20.7	−8.1

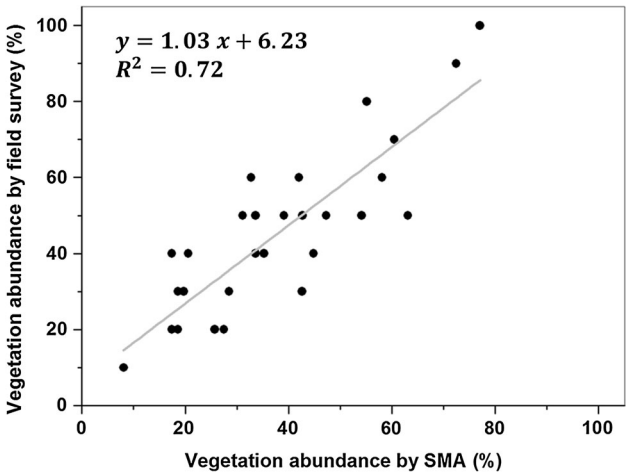

Fig. 6 Relationship of vegetation abundance between field survey and SMA estimation

from the KOMPSAT-2 image. Figure 6 shows a scatter plot illustrating the relationship between the estimated abundance and field-surveyed coverage data at the 29 sites. The scatter plot reveals a strong linear relationship, with R^2 of 0.72, correlation coefficient 0.85, and root mean square error 0.13 (13 %).

There are uncertainties as follows. First, each field survey site covered a small area (0.5 × 0.5 m) relative to a single pixel of the KOMPSAT-2 image (4 × 4 m), even if a highly homogeneous area was selected as a validation site. Second, satellite images and validation field reference data had a 1-month gap. From experience, the area has a strongly variable phenology over short periods, because of meteorological conditions. Third, spectral anomalies should be considered, with spectral characteristics varying by species. Some species do not have an ordinary vegetation spectrum, high reflectance in NIR, which might result in lack of detection with the spectral range of the images used.

Abundance estimation from QuickBird (December 2006)

A QuickBird image from December 2006 was used to remove an unexpected bias from a satellite image acquired

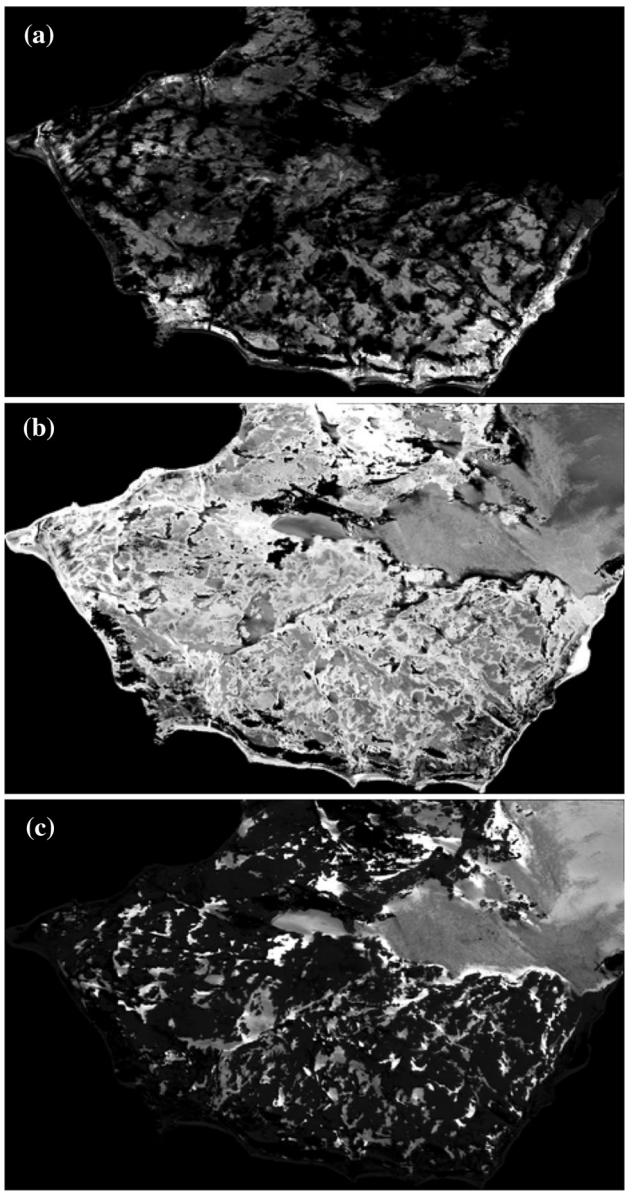

Fig. 7 Estimated abundance image acquired from QuickBird in 2006 as a linear scale 0–1. **a** Vegetation, **b** bare surface, **c** snow

at a certain time. Slowly growing vegetation in polar region allows confirmation of the consistency of results, although QuickBird image was acquired 6 years earlier than the KOMPSAT-2 one. The consistency is described in detail in the following sub-section. Figure 7 shows grayscale abundances of endmembers of (a) vegetation, (b) bare surface, and (c) snow. Vegetation occupied 37 % of the peninsula (Table 2) and showed very high abundance along the southeastern shore. Broad inland areas had low-to-medium abundances of vegetation, except in the northeastern glacier area. Bare surface had 42 %, which was distributed over the entire area with various abundances. This surface showed some abundance in snow-covered areas, which was caused by a layer of water a top melting snow. Snow melt was evidenced by low-to-medium abundance (Fig. 7c), with 21 % abundance over the study area. The summer temperature in 2006 was 2.3 °C, which was 0.7 °C higher than the 25-year average.

Estimated vegetation abundance based on the QuickBird image unfortunately could not be quantitatively validated, because in situ field survey data were unavailable for this image. Estimated abundance was compared using vegetation coverage from a vegetation map (Kim et al. 2007) of the King Sejong Station vicinity. Estimated abundance (by SMA) and coverage (by map) of vegetation were 43 and 47 %, respectively. These data had a time gap between the image and field survey of Kim et al. (2007). The results of both methods show a similar distribution of vegetation between the SMA (Fig. 8a) and vegetation map (Fig. 8b). Therefore, our method allows researchers to acquire both distribution and abundance of vegetation accurately and consistently.

Consistency of distribution and variation of abundance

Distribution and abundance of vegetation were compared to confirm consistency of both results. Figure 9a and b shows extensive very abundant vegetation along the southeastern shore and low-to-mid abundance in inland areas. Vegetation had the same (or similar) distributions (locations), although some areas had different vegetation distributions because of variable snow distributions between 2006 and 2012. Therefore, we infer that polar vegetation growing in certain environments does not change drastically over a short period (Selkirk and Skotnicki 2007). However, interannual variation is shown from the aspect of abundance in Fig. 9. The summer season can be defined from December through February in maritime Antarctica. Generally, February had higher temperatures and less snow coverage than December. Figure 9b (December 2006) shows less snow coverage and higher vegetation abundance than Fig. 9a (February 2012) across the peninsula. This variation is caused by high temperatures and abundant moisture from melting snow. Some studies have reported that mosses and lichens have either activation or increased annual growth rate because of high moisture and temperature (Pannewitz et al. 2003; Sancho and Pintado 2004). Given our result, we believe that vegetation abundance per unit area varies with weather conditions, although the vegetation distribution (location) does not change drastically over short periods.

Discussion

The present study mapped vegetation from two aspects. The first was a first-ever vegetation mapping of the Barton

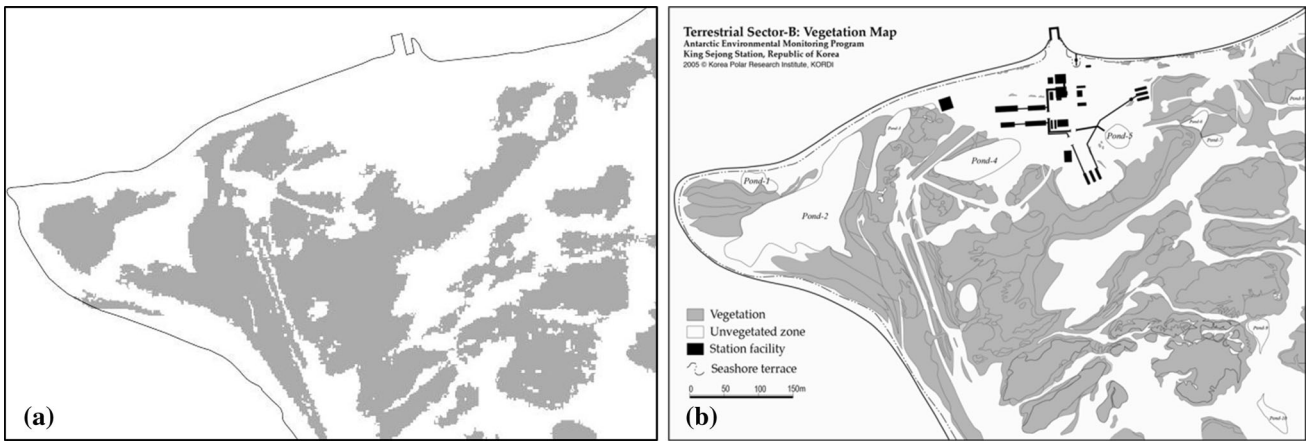

Fig. 8 Distribution of vegetation by (**a**) SMA estimation and (**b**) modified vegetation map by Kim et al. (2007) around King Sejong Station, where, gray color indicates vegetated area

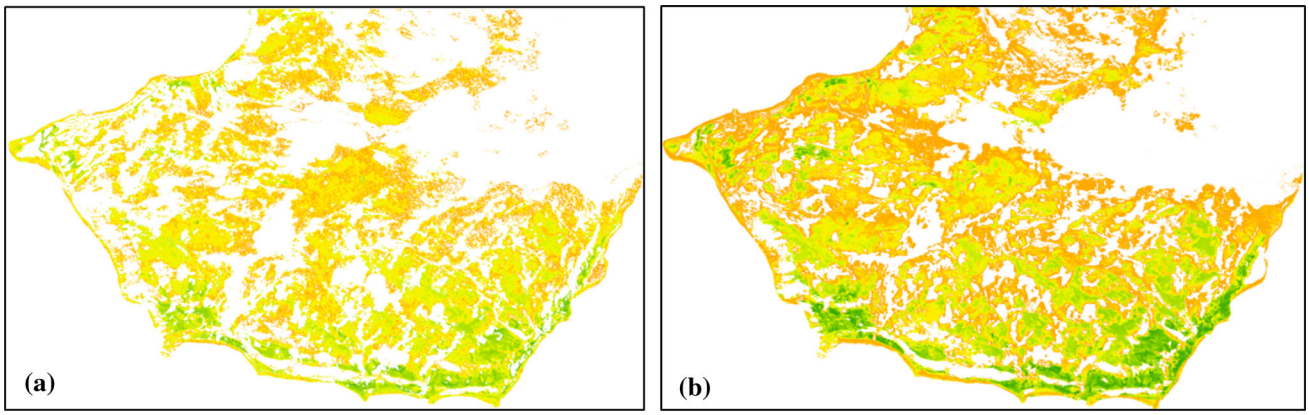

Veg.	**0.0**	**0.0**	**0.1**	**0.2**	**0.3**	**0.4**	**0.5**	**0.6**	**0.7**	**0.8**	**0.9**	**1.0**
B.S.	**0.0**	**1.0**	**0.9**	**0.8**	**0.7**	**0.6**	**0.5**	**0.4**	**0.3**	**0.2**	**0.1**	**0.0**

Fig. 9 Combined abundance map of vegetation and bare surface (B.S.) in (**a**) February 2012 and (**b**) December 2006. Each *color* presents mixture ratios between vegetation and bare surface. *White color* indicates snow or masked shadow area

Peninsula. The second was development of a method for long-term monitoring of vegetation based on satellite image. An SMA method was used to estimate vegetated area for sparse communities of sizes smaller than that of the two high-resolution satellite images used. The estimated vegetation maps frequently showed very high abundance along the southeastern shore and low-to-medium abundance in a nearly snow-free inland area. Estimation accuracies were high, with R^2 of 0.72 from comparison to field data and a 3 % difference from comparison to an existing map. The results showed that vegetation had a consistent distribution and location over 6 years. Vegetation was more abundant in December 2006 than February 2012, although February generally had higher temperatures and less snow coverage than December. This means that there are interannual variations in the aspect of abundance, caused by meteorological conditions. Therefore, more extensive and long-term monitoring based on satellite data is needed for aspects of distribution and abundance.

Given the above, this study produced satellite image-based vegetation maps for broad inaccessible Antarctic tundra, such as the Barton Peninsula study area. The vegetation maps showed high accuracy and consistency and may be used as elementary data for field survey design and monitoring of long-term variation.

In future studies, uncertainties should first be mitigated. These are characterized by differences between field survey and pixel areas, time gaps, and spectral characteristics of species. Second, the potential for species discrimination using remotely sensed imagery should be assessed using

species-specific spectral signatures. Third, it is necessary to investigate relationships between vegetation distribution and various habitat factors, such as elevation, topography, temperature, and moisture. Therefore, simultaneous hyperspectral remote sensing and sufficient or suitable field data are periodically needed, with consideration of both spectral and spatial resolution of remote sensing data. These data should be used to evaluate the potential for biodiversity monitoring via remote sensing, to be used as an indicator of climate change. For the analysis, we need to pay attention to data quality and skill of users in using the method those might affect to result of SMA.

Acknowledgments This study was supported by Korea Polar Research Institute (PE14040 and PE14020) and Korea Aerospace Research Institute (PG14010). Thanks to the anonymous reviewers with helpful comments.

References

Barcikowski A, Gurtowska J (1999) Studies on the biomass of selected species of Antarctic mosses on King George Island, South Shetland Islands, Antarctica. Pol Polar Res 20:283–290

Bergstrom DM, Turner PAM, Scott J, Copson G, Shaw J (2006) Restricted plant species on sub-Antarctic Macquarie and Heard Islands. Polar Biol 29:532–539. doi:10.1007/s00300-005-0085-2

Bhatt US, Walker DA, Raynolds MK, Comiso JC, Epstein HE, Jia G, Gens R, Pinzon JE, Tucker CJ, Tweedie CE, Webber PJ (2010) Circumpolar arctic tundra vegetation change is linked to sea ice decline. Earth Interact 14:1–20. doi:10.1175/2010EI315.1

Bokhorst S, Huiskes A, Convey P, Aerts R (2007) External nutrient inputs into terrestrial ecosystems of the Falkland Islands and the Maritime Antarctic region. Polar Biol 30:1315–1321. doi:10.1007/s00300-007-0292-0

Chen CM, Hepner GF, Forster RR (2003) Fusion of hyperspectral and radar data using the HIS transformation to enhance urban surface features. ISPRS J Photogramm Remote Sens 58:19–30. doi:10.1016/S0924-2716(03)00014-5

Chung H, Lee BY, Chang SK, Kim JH, Kim Y (2004) Ice cliff retreat and sea-ice formation observed around King Sejong Station in King George Island, West Antarctica. Ocean Polar Res 26:1–10

Convey P (2011) Antarctic terrestrial biodiversity in a changing world. Polar Biol 34:1629–1641. doi:10.1007/s00300-011-10068-0

Fretwell PT, Convey P, Fleming AH, Peat HJ, Hughes KA (2011) Detecting and mapping vegetation distribution on the Antarctic Peninsula from remote sensing data. Polar Biol 34:273–281. doi:10.1007/s00300-010-0880-2

Frohn RC, Hinkel KM, Eisner WR (2005) Satellite remote sensing classification of thaw lakes and drained thaw lake basins on the North Slope of Alaska. Remote Sens Environ 97:116–126. doi:10.1016/j.rse.2005.04.022

Furmanczyk K, Ochyra R (1982) Plant communities of the Admiralty Bay region (King George Island, South Shetland Islands, Antarctic). Pol Polar Res 3:25–39

Green AA, Berman M, Switzer P, Craig MD (1988) A transformation for ordering multispectral data in terms of image quality with implications for noise removal. IEEE Trans Geoscience Remote Sens 26:65–74

Green ATG, Sancho LG, Pintado A, Schroeter B (2011) Functional and spatial pressures on terrestrial vegetation in Antarctica forced by global warming. Polar Biol 34:1643–1656. doi:10.1007/s0030-011-1058-2

Jensen JR (2005) Introductory digital image processing: a remote sensing perspective, 3rd edn. Pearson Prentice Hall, New Jersey, pp 431–465

Kennedy AD (1993) Photosynthetic response of the Antarctic moss *Polytrichym alpestre* Hoppe to low temperatures and freeze-thaw stress. Polar Biol 13:271–279

Kim JH, Ahn IY, Hong SG, Andreev M, Lim KM, Oh MJ, Koh YJ, Hur JS (2006) Lichen flora around the Korean Antarctic scientific station, King George Island, Antarctic. J Microbiol 44:480–491

Kim JH, Ahn IY, Lee KS, Chung H, Choi HG (2007) Vegetation of Barton Peninsula in the neighbourhood of King Sejong station (King George Island, maritime Antarctic). Polar Biol 30:903–916. doi:10.1007/s00300-006-0250-2

Kim H, Kim T, Lee H (2012) Brightness value comparison between KOMPSAT-2 images with IKONOS/GEOEYE-1 images. Korean J Remote Sens 28:181–189

Laidler GJ, Treitz PM, Atkinson DM (2008) Remote sensing of arctic vegetation: relations between the NDVI, spatial resolution and vegetation cover on Boothia Peninsula, Nunavut. Arct 61:1–13

Lee BY, Won Y, Oh SN (1997) Meteorological characteristics at King Sejong Station, Antarctica (1988–1996). Report BSPE 97604-00-1020-7. Korea Ocean and Developmental Institute, pp 571–599

Lee JS, Lee HK, Hur J, Andreev M, Hong SG (2008) Diversity of the lichenized fungi in King George Island, Antarctica, revealed by phylogenetic analysis of partial large subunit rDNA sequences. J Microbiol Biotechnol 18:1016–1023

Murray H, Lucieer A, Williams R (2010) Texture-based classification of sub-Antarctic vegetation communities on Heard Island. Int J Appl Earth Obs Geoinfo 12:138–149. doi:10.1016/j.jag.2010.01.006

Okin GS, Roberts DA, Murray B, Okin W (2001) Practical limits on hyperspectral vegetation discrimination in arid and semiarid environments. Remote Sens Environ 77:212–225

Pannewitz S, Schlensog M, Green TGA, Sancho LG, Schroeter B (2003) Are lichens active under snow in continental Antarctica? Ecophysiol 135:30–38. doi:10.1007/s00442-002-1162-7

Pereira AB, Spielmann AA, Martins MFN, Francelino MR (2007) Plant communities from ice-free areas of Keller Peninsula, King George Island, Antarctica. Oecol Bras 11:14–22

Poole I, Hunt RJ, Cantrill DJ (2001) A fossil wood flora from King George Island: ecological implications for an Antarctic Eocene vegetation. Ann Bot 88:33–54. doi:10.1006/anbo.2001.1425

Raynolds MK, Walker DA, Maier HA (2006) NDVI patterns and phytomass distribution in the circumpolar Arctic. Remote Sens Environ 102:217–281. doi:10.1016/j.rse.2006.02.016

Raynolds MK, Comiso JC, Walker DA, Verbyla D (2008) Relationship between satellite-derived land surface temperatures, artic vegetation types, and NDVI. Remote Sens Environ 112:1884–1894. doi:10.1016/j.rse.2007.09.008

Robin M, Chapuis JL, Lebouvier M (2011) Remote sensing of vegetation cover change in islands of the Kerguelen archipelago. Polar Biol 34:1689–1700. doi:10.1007/s00300-011-1069-z

Robinson SA, Wasley J, Tobin AK (2003) Living on the edge-plants and global change in continental and maritime Antarctica. Glob Chang Biol 9:1681–1717

Sancho LG, Pintado A (2004) Evidence of high annual growth rate for lichens in the maritime Antarctic. Polar Biol 27:312–319. doi:10.1007/s00300-004-0594-4

Selkirk PM, Skotnicki ML (2007) Measurement of moss growth in continental Antarctica. Polar Biol 30:407–413. doi:10.1007/s00300-006-0197-3

Stow DA, Hope A, McGuire D, David V, Gamon J, Huemmrich F, Houston S, Racine C, Sturm M, Tape K, Hinzman L, Yoshikawa K, Tweedie C, Noyle B, Silapaswan C, Douglas D, Griffith B, Jia G, Epstein H, Walker D, Daeschner S, Petersen A, Zhou L, Myneni R (2004) Remote sensing of vegetation and land-cover change in Arctic Tundra Ecosystems. Remote Sens Environ 89:281–308. doi:10.1016/j.rse.2003.10.018

Théau J, Peddle DR, Duguay CR (2005) Mapping lichen in a habitat of Northern Quebec, Canada, using an enhancement-classification method and spectral mixture analysis. Remote Sens Environ 94:232–243. doi:10.1016/j.rse.2004.10.008

Torres-Mellado GA, Jaña R, Cassanova-Katny MA (2011) Antarctic hairgrass expansion in the South Shetland archipelago and Antarctic Peninsula revisited. Polar Biol 34:1679–1688. doi:10.1007/s00300-011-1099-6

Victoria FC, Pereira AB, Da Costa DP (2009) Composition and distribution of moss formations in the ice-free areas adjoining the Arctowski region, Admiralty Bay, King George Island, Antarctica. Iheringia Sér Bot 64:81–91

Xie Y, Sha Z, Yu M (2008) Remote sensing imagery in vegetation mapping: a review. J Plant Ecol 1:9–23. doi:10.1093/jpe/rtm005